Received: 24 June 2025 | *Revised: 26 August 2025* | *Accepted: 28 August 2025* | *Vol. 1 | Issue 2| December 2025*
e-ISSN: 3105-2169

International Journal of Mechatronics, Robotics, and Artificial Intelligence
Original Article

Numerical Investigation of Temperature Distribution and Thermal Resistance in a Heat Sink Using Varied Fin Radius and Length

Sana J. Yaseen *[1], **Ali A. Abed**[1], **Abdel-Nasser Sharkawy**[2,3]
[1]Mechatronics Engineering Department, University of Basrah, Basrah, Iraq
[2]Mechatronics Engineering, Mechanical Engineering Department, Faculty of Engineering, South Valley University, Qena 83523, Egypt
[3]Mechanical Engineering Department, College of Engineering, Fahad Bin Sultan University, Tabuk 47721, Saudi Arabia

Correspondence
* Sana Jaafar Yaseen
Mechatronics Engineering Department, University of Basrah, Basrah, Iraq
Email: sana.yaseen@uobasrah.edu.iq

Abstract

This research provides a numerical investigation into the thermal and hydraulic performance of a pin-fin heat sink, considering the effects of fin radius, fin length, and the arrangement of the arrays. A 3D computational model was developed and solved in ANSYS Icepak for conjugate heat transfer and fluid flow under forced convection. The fin length was changed from 1 cm to 8 cm, and the fin radius from 1 mm to 6 mm. Inline and staggered configurations were investigated for the two types of arrangements to assess their effect on performance. The findings underscore an important trade-off between thermal resistance and pressure drop. As anticipated, the staggered configuration provided a consistent increase in the heat transfer coefficient because of better flow mixing and disruption of the thermal boundary layers. This improvement, however, came with a significantly higher pressure drop. From the analysis, it was evident that the best configuration is strongly influenced by the length of the fins. With shorter fins of 1-3 cm, the staggered array decreased thermal resistance far better than the in-line array. With longer fins of 6-8 cm, the in-line configuration frequently provided better overall performance because the mass flow rate was higher due to less pressure drop than the long, staggered path. In addition, the radius of the fin exhibited a nonlinear relationship with regard to performance. Increasing the radius provided a greater area for heat dissipation, but it also increased obstruction to the flow. For every specific length and arrangement combination, a thermal performance maximizing radius existed. This work gives important design rules for the thermal optimization of the heat sink geometry and emphasizes the importance of the staggered array, for short fin lengths, while revealing the in-line configuration advantage for long fin lengths when minimizing pressure drop becomes the main concern.

Keywords

Numerical investigation, Heat sink, Pin fin, Maximum temperature, Thermal resistance, Electronic cooling

I. INTRODUCTION

Progress in electronic chip technology has reached a stage where significantly powerful chips can now be accommodated in more compact packages [1]. Consequently, the increased power density of these devices has made it imperative to implement more efficient thermal management solutions to prevent them from exceeding the maximum allowable operating temperature. To mitigate heat dissipation from components, fins made of highly thermally conductive materials can be incorporated [2][3].

To improve the system's effective thermal conductivity, fins made of highly conductive materials, such as aluminum, were introduced. Consequently, the addition of fins results in increased thermal conductivity, albeit at the expense of some latent heat storage [4][5]. In the improvement of electronic device cooling, heat sinks are used to achieve optimal cooling function in the electronics industry [6]. The challenge for designers is to effectively dissipate the heat generated by the component while maintaining the component temperature at the level necessary to ensure reliable system operation [7]. Over the past two decades, researchers have devised a solution to improve heat dissipation by using different forms of micro-fin heat sinks [8][9]. The goal is to achieve the most efficient cooling for the designed system, considering both cost and size. To this end, various geometries were investigated to evaluate the influence of heat sink design on cooling. Jalal et al. [10] The impact of micro pin fins on thermal performance was numerically investigated. Several fin configurations, including in-line and staggered fins, were analyzed. The results indicated an improvement in cooling performance from 7.9% to 9.3% with increasing fin count from 902 to 1312, and an improvement from 10.2% to 11.1% with increasing fin count from 902 to 1640.

Ekpu [11] The influence of fin arrangement on the thermal performance of microelectronic devices was studied using ANSYS finite volume design software. The results clearly demonstrated that the heat sink fin configuration significantly influences both the thermal resistance and overall efficiency of the microelectronic device. Furthermore, the rectangular fin configuration showed advantages over the other configurations studied. Tanda [12] An experimental investigation was conducted to explore heat transfer and pressure drop in a rectangular channel equipped with diamond-shaped fin arrays. The study investigated both in-line and staggered fin arrangements. The results demonstrated that the incorporation of diamond-shaped fins resulted in improved heat transfer compared to an un-finned rectangular channel. This improvement reached a maximum of 4.4 times when maintaining a constant mass flow rate and 1.65 times when maintaining constant pumping power. Shatikian et al. [13] conducted a numerical investigation focusing on a design with internal fins with exposed tips, allowing contact with the surrounding air. In their study, they varied both the fin thickness and the proportion of the fins exposed to the surrounding air. The computational results indicate that the transient phase change process, quantified by the volumetric melt fraction of the PCM, is influenced by the thermal and geometric characteristics of the system, including the thickness and exposed portion of the fins.

Yang and Peng [14] used the SIMPLE computational fluid dynamics algorithm to solve the Navier-Stokes equations to study the thermal and hydraulic performance of composite heat sinks and compare them with plate-fin heat sinks. They found that the thermal resistance of pure plate-and-fin heat sinks was higher than that of composite, which included plate fins with some pins between the plates. Abdelmohimen et al. [15] used CFD to compare impinging and parallel flow according to the thermal output performance, pressure drop, and efficiency. They prepared the slides cutting fins off plate heat sinks to produce configurations of one, two, three, and four slides. They indicated that the impinging flow gives better thermal resistance than parallel flow for all configurations. Zhou and Catton [16] used a 3D CFD model based on the Reynolds-averaged Navier-Stokes equations to examine the energy dissipation and pressure drop of 22 different finned plate heat sinks. They found through numerical analysis that the elliptical fin heat sink outperforms all other varieties of pin fin heat sinks. Additionally, statistical approaches were used to study the effect of fin arrangement method on thermal resistance and pressure drop.

The current research work analyzes the effect of fin geometry on the heat dissipation generated by heat sinks using ANSYS-Icepak software. The purpose of this study was to compare and study their effect on heat transfer rates, with the aim of determining the best and most effective fin radius, fin length for use in various circuit boards. The results obtained included the cooling performance of each heat sink, maximum temperature and the thermal resistance which were selected as performance indicators. The importance of this research lies in its ability to provide clear recommendations for choosing the appropriate fin radius and length for two fin arrangements in-line and staggered array when designing effective heat sinks.

II. The Physical Model

In this research, a heat sink with 25 fins of circular cross-sections (pin fin) was studied. A schematic diagram of the heat sink is presented in Fig. 1. The model used is a rectangular duct containing a heat sink mounted on an electronic heat source (chip). The heat sink is made of aluminum 6063- T5 which has properties of k=167 W/mK and air is used as the cooling fluid. The total power is set to 20W was applied by a heat source located at the bottom of the heat sink, and the heat sink dimensions are given in Table I. All the walls of the heat sink are insulated except of two regions (the entrance, which is air as cooling fluid, with a known speed and temperature) and (the exit, which is exposed to atmospheric pressure).

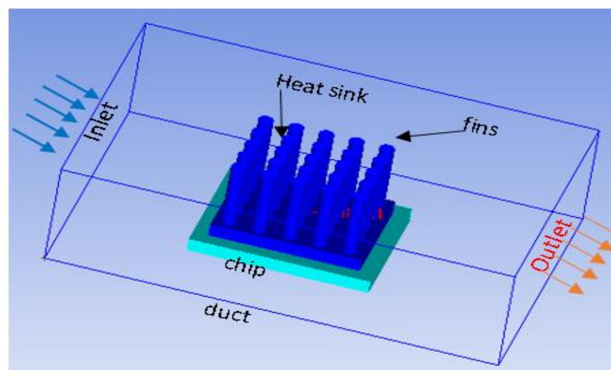

Fig. 1. Schematic diagram of the present study

TABLE I.
GEOMETRIC DIMENSIONS OF THE ENTIRE DOMAIN

Parameter	Dimensions (cm)	
Rectangular duct	30x20x8	
Source (chip)	12x10x1	
Heat Sink	10 x 8 x 1 cm	
Fins	Number of fins=5	
Base Height, overall height	1, 6	
Cross Section	Circular	With radius (R) varying from 1 to 6 mm

III. THE NUMERICAL ANALYSIS

A numerical analysis is conducted using the ANSYS-Icepak software to assess the cooling of a heat sink, and air is used as the coolant fluid. The Icepak software relies on the ANSYS FLUENT solver to provide calculations of the thermal and fluid flow tasks and to create a diagram, add boundary conditions, and extract graphics and values for all studied cases. Heat transfer in the heat sink unit is a conjugate process, which combines conduction heat transfer in the solid parts and convection heat transfer through the fluid.

A. *Assumptions*

The simulation utilizes the 3D Navier-Stokes and energy equations, in addition to mass conservation, to model temperature and flow fields. This involves the application of simplifying assumptions to the momentum and energy equations. The assumptions are as follows:

1) 3D, incompressible, laminar, and steady-state flow condition is assumed.
2) There will be no slip flow close to the walls.
3) The viscous dissipation in the energy equation is negligible.
4) The radiation is negligible.
5) The effect of gravity is negligible.
6) Constant fluid and solid properties.

After applying this set of assumptions, the 3D equation system that governs the single-phase model includes the continuity, momentum, and energy equations, which can be described as [17]:

$$\frac{\partial u}{\partial x}+\frac{\partial v}{\partial y}+\frac{\partial w}{\partial z}=0 \tag{1}$$

Momentum in x, y and z directions, respectively are:

$$u\frac{\partial u}{\partial x}+v\frac{\partial u}{\partial y}+w\frac{\partial u}{\partial z}=-\frac{1}{\rho}\frac{\partial P}{\partial x}+\frac{\mu}{\rho}\left(\frac{\partial^2 u}{\partial x^2}+\frac{\partial^2 u}{\partial y^2}+\frac{\partial^2 u}{\partial z^2}\right) \tag{2}$$

$$u\frac{\partial v}{\partial x}+v\frac{\partial v}{\partial y}+w\frac{\partial v}{\partial z}=-\frac{1}{\rho}\frac{\partial P}{\partial y}+\frac{\mu}{\rho}\left(\frac{\partial^2 v}{\partial x^2}+\frac{\partial^2 v}{\partial y^2}+\frac{\partial^2 v}{\partial z^2}\right) \tag{3}$$

$$u\frac{\partial w}{\partial x}+v\frac{\partial w}{\partial y}+w\frac{\partial w}{\partial z}=-\frac{1}{\rho}\frac{\partial P}{\partial z}+\frac{\mu}{\rho}\left(\frac{\partial^2 w}{\partial x^2}+\frac{\partial^2 w}{\partial y^2}+\frac{\partial^2 w}{\partial z^2}\right) \tag{4}$$

Energy equation:

$$u\frac{\partial T}{\partial x}+v\frac{\partial T}{\partial y}+w\frac{\partial T}{\partial z}=\frac{k}{\rho\, Cp}\left(\frac{\partial^2 T}{\partial x^2}+\frac{\partial^2 T}{\partial y^2}+\frac{\partial^2 T}{\partial z^2}\right) \tag{5}$$

The variables "T" and "P" represent the fluid temperature and pressure, whereas u, v, w, ρ, μ, C_p and k represent the fluid velocity components, density, dynamic viscosity, specific heat capacity and thermal conductivity, respectively. The equation of the energy equation for the solid walls, is given by [18]:

$$\frac{\partial^2 T_s}{\partial x^2}+\frac{\partial^2 T_s}{\partial y^2}+\frac{\partial^2 T_s}{\partial z^2}=0 \tag{6}$$

where, *'s'* refers to the solid region.
The maximum temperature difference can be calculated by the equation [19]:

$$\Delta T_{max}=T-T_{in} \tag{7}$$

Where T, the heat source temperature, T_{in} is the inlet temperature

$$R_{th}=\Delta T_{max}/Q \tag{8}$$

Where R_{th} the thermal resistance in (°C/W), where Q is the power supplied, which is equal to 20 W.

B. *Boundary Conditions*

The boundary conditions (BC) for this problem are stated as follows. The air is uniformly induced with a constant temperature and velocity at inlet portion of the rectangular duct. At the downstream boundary of the computational domain, which is located at the outlet of the duct in X-direction, a pressure boundary condition is employed. No slip conditions with thermal insulation are provided on all the other confined walls. At the bottom of the heat sink, a uniform constant heat flux is applied from the source heat. The adiabatic thermal boundary conditions are utilized at the outer perimeter of the base of the heat sink except for the heated area. These boundary conditions (BC) are presented as follows:

1) BC for the flow field: uniform velocity at the inlet of channel. No-slip condition is used for all the walls, i.e., $u=0$, $v=0$, $w=0$.
2) Adiabatic boundary conditions are applied to all the boundaries of the solid region except for the heat sink bottom wall, where a heat source with constant power is applied. The power is 20W.

At the inlet, the temperature $T=T_{in}=20\,°\mathrm{C}$, $v_{in}=1\frac{m}{s}$, $-k_s\frac{\partial Ts}{\partial y}=-k_f\frac{\partial Tf}{\partial y}$ at the fluid–solid interface, $\frac{\partial T}{\partial y}=0$ at the outlet.

C. *Verification of Grid Independence*

Mesh independence testing (mesh convergence testing) is a systematic computational process used in numerical simulations to ensure that calculation results are not affected by the number of elements or cells in the mesh. This test demonstrates that a sufficiently optimized mesh gives an accurate answer, without being so optimized that it requires too long to complete the test. Grid independent is carried out to ensure the accuracy of the current numerical results. In this study, a HEXA-dominant mesh was generated in the preprocessing module. The grid independence test is first conducted by using several different numbers of elements and nodes. The computational mesh of the heat sink model is shown in Fig. 2. The results obtained from these meshes are summarized in Table II.

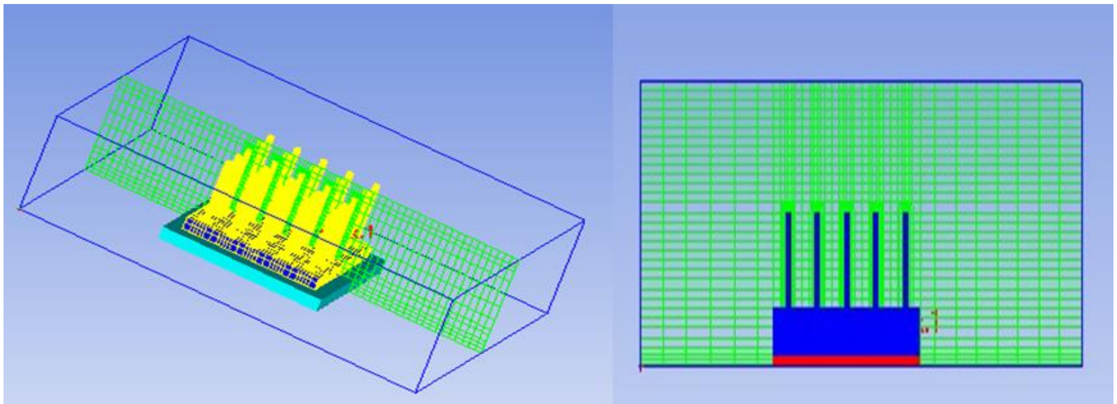

Fig. 2. The computational mesh of the heat sink model. The left side of Figure shows an overview of the entire domain, whereas the right side presents a detailed side view of the mesh surrounding the fins.

TABLE II.
THE NUMBER OF NODES, ELEMENTS, AND MAXIMUM TEMPERATURE.

Test No.	Number of Elements	Number of Nodes	Maximum Temperature (°C)
1.	37944	35216	38.8219
2.	45273	41600	38.1847
3.	47616	43840	37.9748
4.	52359	48480	37.9447
5.	84984	80576	37.9447

As can be shown from Table II that increasing the number of cells beyond 47616 results in a negligible temperature variation of less than 0.04%. Beyond this point, further grid refinement does not appreciably impact the solution. As a result, the fourth mesh size is selected for calculations across all fin geometries to maintain maximum accuracy.

D. Discussion

Validation of the results with previous work of Rosli et al. [20], the temperature and airflow for circular in-line arrangement (CIA) of 6 rows and 6 columns of pin fin heat sink models can be shown in Table III, where all pin fin is arranging uniformly with a 0.4 cm distance between the pin fins for CIA in line arrangement model. From comparing temperatures for model CIA in line arrangement model with present results, it can be noticed that the error percentage between the present results and the ref [20] is 0.898%.

TABLE III.
VALIDATION OF THE RESULTS COMPARED WITH REF [20].

Arrangement	Source Temp [20]	Source Temp (Current Study)	error %
In-line (CIA)	107.43°C	106.474°C	0.898

IV. THE SIMULATION RESULTS

A. Temperature Distribution along the heat sink

In thermal management systems, especially in electronic heat sink, it is crucial to consider the significant consequences of both high and low temperatures. Higher temperatures can result in reduced efficiency and the risk of electronic component failure, whereas lower temperatures typically indicate efficient heat dissipation. Therefore, analyzing the temperature distribution within the sink provides essential information about the effectiveness of the cooling system in use.

Fig. 3 illustrates the temperature distribution inside a heat sink, with a clear gradient from the cooler inlet area of the rectangular duct to the warmer outlet area. This gradient indicates the gradual heating of the cooled air as it absorbs heat from the heat source below it.

The temperature increase corresponds to the direction of air flow, supporting the understanding of convective heat transfer. The incoming air at the duct entrance is cool and absorbs heat efficiently. As it moves through the duct, its temperature increases, making it less efficient at removing heat.

Starting with the fins, as shown in the figure, a 5 mm radius drawing shows the side view of the channel with a plane cut parallel to the x-axis and passing through the center basin (the fins are cut in two). The temperature distribution pattern shows a gradual transition from the cooler inlet region, which registers around 19.9 °C, to higher maximum temperatures, peaking between 37.8 and 43.8 °C, depending on the fin radius.

It is also evident that the highest temperature is at the base of the fin, gradually decreasing towards the tip due to thermal conduction from the heat source to the fins. This decline suggests that while the fin bases effectively conduct heat away from the source, the tips of the fins may not be as efficient in dissipating this heat into the surrounding air.

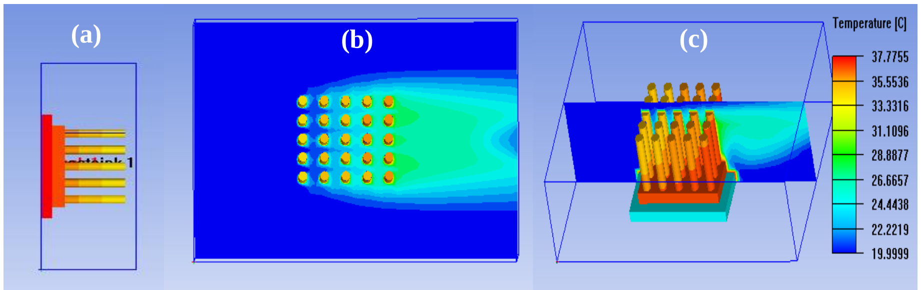

Fig. 3. Temperature distribution along the heat sink at R = 5 mm (a) side view (b) upper view (c) 3D view.

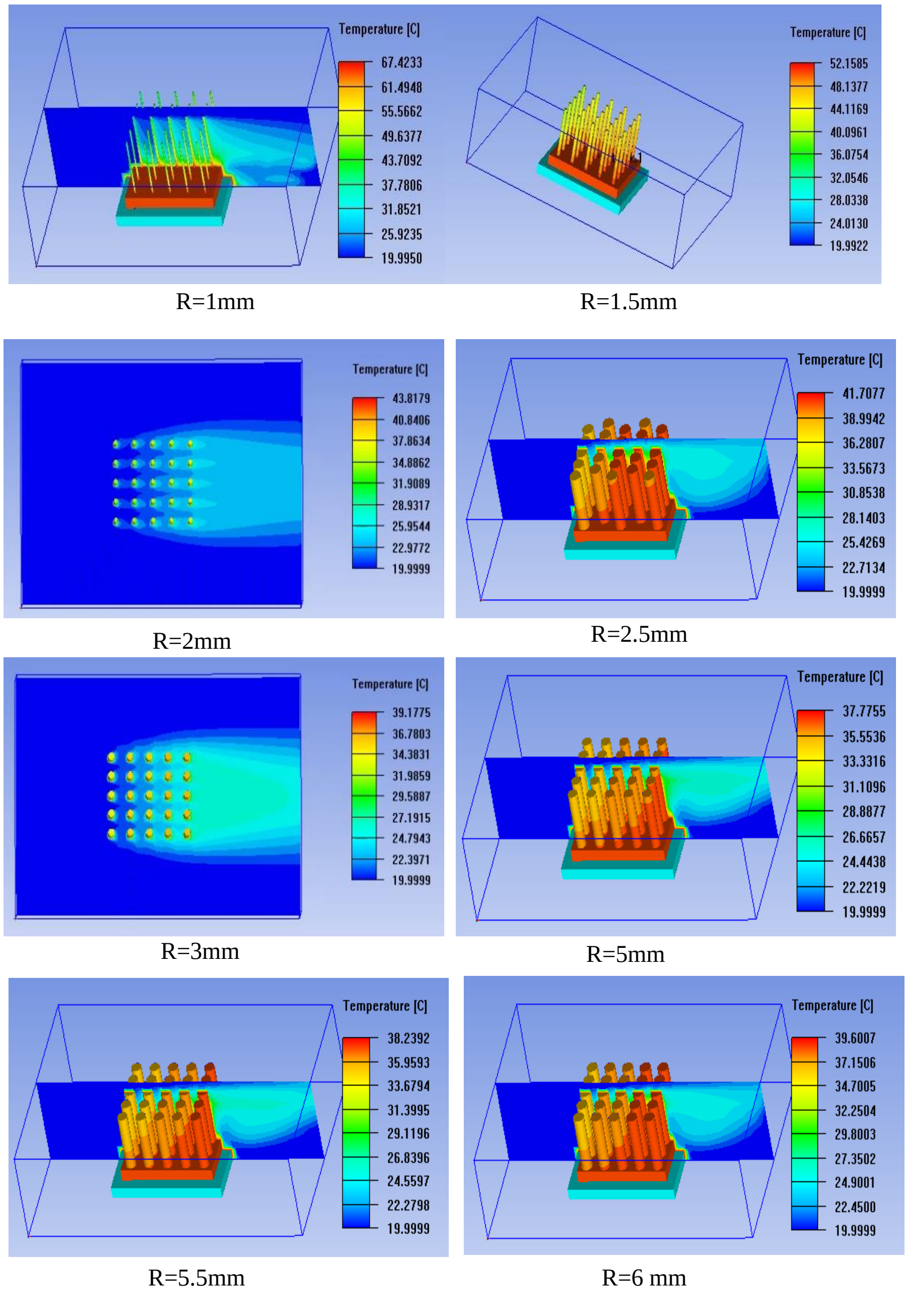

Fig. 4. Temperature distribution along the duct's components at different R.

B. Temperature Distribution of Different Fin Radius (R)

Fig. 4 shows a 3D temperature plot of the heat sink and fins at different fin radii, with the highest temperature recorded at approximately 52°C when the fin radius was 1 mm. The lowest temperature was recorded when the fin radius was 5mm. Note that increasing the radius increases the surface area in contact with the cooling air, enhancing efficient convective heat transfer. This is reflected in the relatively cool temperatures observed throughout the heat sink.

Fig. 5 represents the relation between maximum temperature observed at the heat sink draw verse the different values of fin radii. It can be shown that as R increases, the T_{max} reduces till it reaches R=5 mm T_{max} will be the lowest value. Beyond this value of R, the maximum temperature increased. This belongs to as R increases the surface area of fins increase so the heat convention from fins increases which leads to reduces the T_{max}. While as R increases beyond 5mm the space between fins reduces results in reduces the heat transfer between the fins and the passing air, so the T_{max} increases.

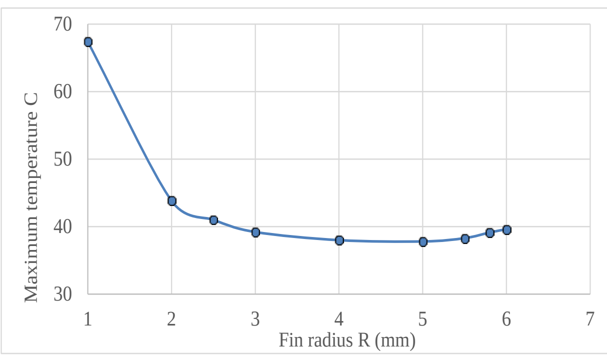

Fig. 5. Maximum temperature along the heat sink at different R.

C. Thermal Resistance (R_{th})

The effect of increases of R on the thermal resistance can be shown in Fig. 6. It can be shown that minimum R_{th} occurs at R=5mm, while increases R led to reduced surface contact area with the passing air so R_{th} increase. It can be concluded that the best value of fin radius (R) is 5mm.

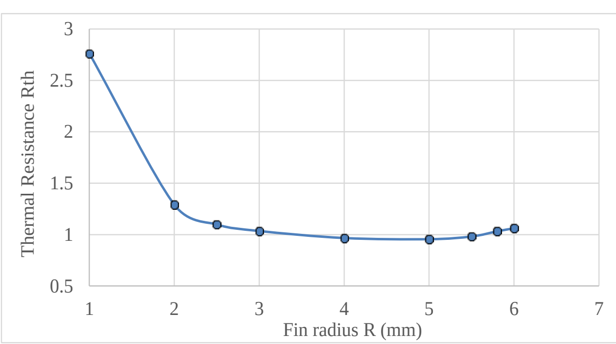

Fig. 6. Thermal resistance along the heat sink at different R.

D. Effect of Fin arrangement

The distribution of fins whether arranged in a straight line or arranged in a staggered plays a key role in shaping the overall thermal performance of the heat sink.

1) In–line arrangement

The fins in this design extend in parallel lines. Under normal operation the airflow acts like a smooth ribbon of air gliding through the spaces between the vertical elements. A laminar boundary layer appears at each fin face: the velocity climbs from zero at the metal surface and then merges into free-stream velocity somewhere within the open channel. Heat must cross this relatively stagnant layer before the air it touches is carried downstream. As the air warms, its effectiveness is diluted, and each succeeding row of fins modulates the thermal load. The stagnant air the downstream fins face appears less and less capable of efficient heat removal, and consequently the maximum sink temperature rises.

2) In-staggered arrangement

Fins in this design are arranged so that each new row is staggered. This sort of offset denies the airflow a smooth, straight discovery of the passage: the stream must crumple against each second-row fin and then twist into a new channel, a mechanical rapid-weaving of the flow. Such rapid changes break and thin the boundary layer, never allowing it to develop a quiet thick cushion of less energetic air. As that layer crumbles the fin surface is challenged by fresh, high-velocity moving air. The airflow reorganizes exposure time across the entire facing perimeter, shortening thermal time constants and elevating local heat-transfer rates. The fins cool more uniformly and the overall maximum sink temperature is lowered.

Temperature distribution along the heat sink is investigated with fin arrangement (in-line and staggered) at radius R=5mm and fin length L_f = 6 cm, as shown in Fig. 7.

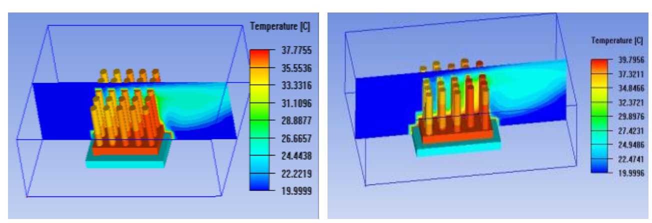

(a) (b)

Fig. 7. Temperature distribution along the heat sink with fin arrangement (a) in-line (b) staggered at R=5mm L_f= 6 cm.

E. Effect of Fin length on maximum temperature and thermal resistance

Fig. 8 and Fig. 9 show the effect of length of fin (L_f) on the maximum temperature (T_{max}) and thermal resistance (R_{th}) respectively at two arrangements of fins. It shows that increasing fin length for a fixed-base heatsink, initially reduces the maximum temperature (improving performance), but beyond a certain height (6 cm) as shown in Fig. 8 the benefit becomes negligible at (L_f=7 and 8 cm), which means that beyond that height yields little to no benefit. Also, Fig. 9 shows how increasing fin length decreases thermal resistance. Beyond an optimal length (6 cm), the benefit diminishes drastically, and further increases in length provide almost no reduction in thermal resistance. The reason of this behavior the fin increases the surface area available for heat transfer to the surrounding fluid (usually air). A taller fin simply has more surface area from its base to tip. This allows more heat to be convicted away from the heat sink.

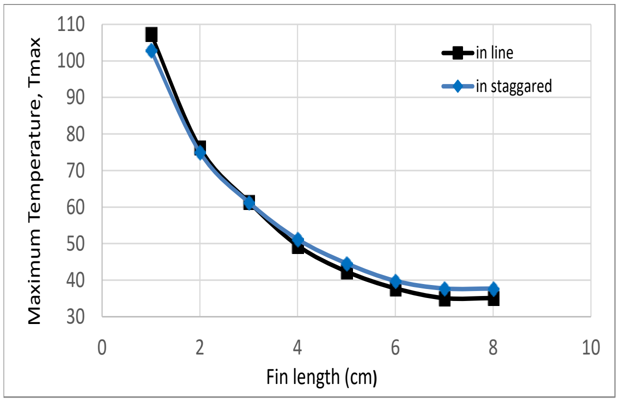

Fig. 8. Maximum temperature along the heat sink vs. fin length at different fin arrangement.

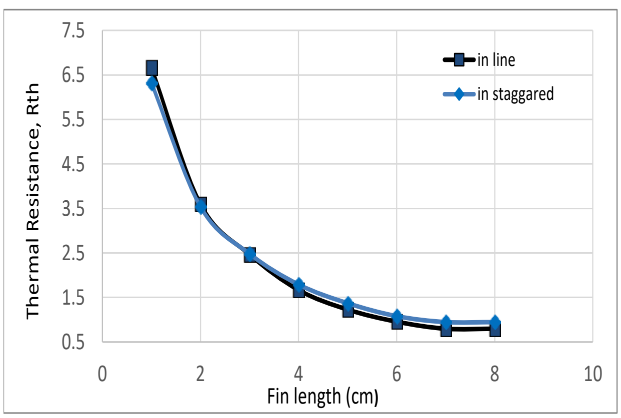

Fig. 9. Thermal resistance along the heat sink vs. fin length at different fin arrangement

F. Effect of Fin arrangement on maximum sink temperature, thermal resistance and pressure drop

Fig. 8 and Fig. 9 show the effect of fin arrangement on maximum sink temperature and thermal resistance distribution along the whole heat sink. It can be noticed from these Figures that a staggered fin arrangement results in a lower maximum temperature and lower thermal resistance than an in-line arrangement for the same airflow and base area at fin length smaller than 3cm, after this length in –line fins gave smaller values of T_{max} and R_{th}. Short staggered fins have high heat transfer coefficient, which give the lowest T_{max} and R_{th}, while when it became longer it has high pressure drop which results in low mass flow rate that results in high values of T_{max} and R_{th}. In case of in-lines arrangement fins, at high length can become superior because its lower flow resistance maintains a much higher mass flow rate, which results in increasing the heat transfer that gives lower values of T_{max} and R_{th}. From Figs. 8 and 9, the value of fin length that gives the same values of T_{max} and R_{th} for the two arrangement of fins is L_f=3 cm.

The effect of Fin arrangement on pressure drop can be seen in Fig.10, which draws for R=5 cm, L_f=3 cm for different fins arrangements. From this Figure, it is clear that fin In-Line arrangements have lower pressure drop than in staggered arrangement. Since in staggered the flow path increases, the pressure drop accumulates, leading to a very high total pressure drop, which reducing the mass flow rate that results in reducing heat transfer and increasing T_{max} and R_{th} so the staggered array's advantage can reverse at longer fins. While in-line array has lower pressure drop due to short flow path.

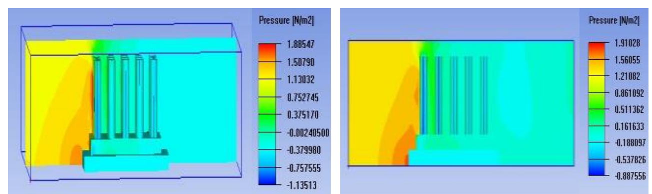

(a) (b)

Fig.10. Pressure distribution along the heat sink at different fin arrangement (a) in line (b) staggered.

V. CONCLUSIONS

In this study, the effect of fin radius, length and arrangement on heat sink performance were investigated. Evaluation of the cooling effectiveness of each heat sink relied on comprehensive performance indicators, including maximum temperature reduction and thermal resistance across the heat sink also pressure drop. The combination of these parameters allowed us to evaluate the thermal performance of each design. The key findings of this research are as follows:

1) Fin shape is a key factor in determining the temperature and thermal resistance of the heat sink.
2) There is a specific radius where the maximum temperature and the thermal resistance is at its lowest possible value. For the size of the heat sink considered in this study, the optimal radius is 5 mm.
3) For a given size and airflow, switching from an in-line to a staggered fin distribution will reliably lower the heat sink's maximum temperature. The improvement can be substantial, often on the order of 10-20% or more. However, this comes at the cost of increased pressure drop, which must be matched with an appropriate fan.
4) Fin length is a powerful design lever, but its effect is subject to strong diminishing returns. The goal is not to increased length, but to find the optimal length that minimize the maximum temperature and thermal resistance.

For the future work, the current heat sink design could be modified by studying other fin shapes such as longitudinal and cylindrical, making the fins more randomly distributed, or changing its design to a cubic heat sink with petrified pin fins.

NOMENCLATURE

Symbol	Meaning	Symbol	Meaning
X, Y, Z	Coordinate components	U, V, W	Dimensionless velocity components
Q	Power (W)	μ	viscosity
R_{th}	Thermal resistance	s	solid
L_f	length of the fin	f	fluid
T_{max}	Maximum Temperature	R	Fin radius

CONFLICT OF INTEREST

One of the authors, Prof. Dr. Ali Ahmed Abed, is the Editor-in-Chief of the International Journal of Mechatronics, Robotics, and Artificial Intelligence (IJMRAI). To ensure transparency and avoid any potential conflict of interest, he was not involved in the editorial processing or peer review of this manuscript. The review process was handled independently by other qualified editors.
The authors have no conflict of relevant interest to this article.

REFERENCES

[1] W. Luo, L. Cao, Y. Shi, L. Wan, H. Zhang, S. Li, G. Chen, Y. Li, S. Li, Y. Wang, S. Sun, M. F. Karim, H. Cai, and A. Liu, "Recent progress in quantum photonic chips for quantum communication and internet," *Light: Science and Applications*, vol. 12, no. 1. Springer Nature, 2023, doi: 10.1038/s41377-023-01173-8

[2] S. Al-Omari, Z. Qureshi, E. Elnajjar, and F. Mahmoud, "A heat sink integrating fins within high thermal conductivity phase change material to cool high heat-flux heat sources," *International Journal of Thermal Sciences*, vol. 172, 2022, doi: 10.1016/j.ijthermalsci.2021.107190

[3] A. Gaikwad, A. Sathe, and S. Sanap, "A design approach for thermal enhancement in heat sinks using different types of fins: A review," *Frontiers in Thermal Engineering*, vol.2, 2023, doi: 10.3389/fther.2022.980985

[4] T. Yang, W. P. King, and N. Miljkovic, "Phase change material-based thermal energy storage," *Cell Reports Physical Science*, vol. 2, no. 8. Cell Press, 2021, doi: 10.1016/j.xcrp.2021.100540

[5] M. B. Ben Hamida, K. Hajlaoui, and M. A. Almeshaal, "A 3D numerical analysis using phase change material for cooling circular light emitting diode," *Case Stud. Therm. Eng.*, vol. 43, no. February, p. 102792, 2023, doi: 10.1016/j.csite.2023.102792

[6] M. Ben Hamida, "Thermal management of square light emitting diode arrays: modeling and parametric analysis," *Multidiscip. Model. Mater. Struct.*, vol. 20, no. 2, pp. 363–383, 2024, doi: 10.1108/MMMS-09-2023-0311

[7] H. Shafeie, O. Abouali, K. Jafarpur, and G. Ahmed, "Numerical study of heat transfer performance of single-phase heat sinks with micro pin-fin structures." *Applied Thermal Engineering*, Vol. 58, no. 1-2, pp. 68-76, 2013, https://doi.org/10.1016/j.applthermaleng.2013.04.008

[8] T. Yeom, T. Simon, T. Zhang, M. Zhang, M. North, and T. Cui, "Enhanced heat transfer of heat sink channels with micro pin fin roughened walls." *International Journal of Heat and Mass Transfer*, Vol. 92, pp. 617-627, 2016 https://doi.org/10.1016/j.ijheatmasstransfer.2015.09.014

[9] W. Arshad, and H. M. Ali. "Graphene Nano platelets Nano fluids thermal and hydrodynamic performance on integral fin heat sink." *International Journal of Heat and Mass Transfer*, vol. 107, pp. 995-1001, 2017, https://doi.org/10.1016/j.ijheatmasstransfer.2016.10.127

[10] J. M. Jalil, A. H. Reja, and A. M. Hadi. "Numerical Investigation of Thermal Performance of Micro-Pin Fin with Different Arrangements." *IOP Conference Series: Materials Science and Engineering*. vol. 765. no. 1. IOP Publishing, 2020, doi: 10.1088/1757-899X/765/1/012037.

[11] M. Ekpu, "Effect of Fins Arrangement on Thermal Performance in Microelectronics Devices." *Journal of Applied Sciences and Environmental Management*, vol.22, no.11, pp.1797-1800, 2018, doi: 10.4314/jasem.v22i11.14.

[12] G. Tanda, "Heat transfer and pressure drop in a rectangular channel with diamond-shaped elements." *International Journal of Heat and Mass Transfer*, vol. 44, no. 18, pp. 3529-3541, 2001, https://doi.org/10.1016/S0017-9310(01)00018-7.

[13] V. Shatikian, G. Ziskind, and R. Letan, "Numerical investigation of a PCM-based heat sink with internal fins," *Int J Heat Mass Transf*, vol. 48, no. 17, pp. 3689–3706, 2005, doi: 10.1016/j.ijheatmasstransfer.2004.10.042.

[14] Y. T. Yang and H. Sen Peng, "Numerical study of thermal and hydraulic performance of compound heat sink," *Numeri Heat Transf A Appl*, vol. 55, no. 5, 2009, doi: 10.1080/10407780902776405.

[15] M. A. H. Abdelmohimen, K. Almutairi, M. A. Elkotb, H. E. Abdelrahman, and S. Algarni, "Numerical Investigation of using Different Arrangement of Fin Slides On the Plate-Fin Heat Sink Performance," *Thermal Science*, vol. 25, no. 6, 2021, doi: 10.2298/TSCI201004065A.

[16] F. Zhou and I. Catton, "Numerical evaluation of flow and heat transfer in plate-pin fin heat sinks with various pin cross-sections," *Numeri Heat Transf A Appl*, vol. 60, no. 2, 2011, doi: 10.1080/10407782.2011.588574.

[17] S. J. Yaseen. "Numerical study of the fluid flow and heat transfer in a finned heat sink using Ansys Icepak", *Open Engineering*, vol. 13, no. 1, 2023, pp. 20220440. https://doi.org/10.1515/eng-2022-0440.

[18] M. Izadi, H. Fagehi, A. Imanzadeh, S. Altnji, M. Bechir Ben Hamida, and M. A. Sheremet, “Influence of finned charges on melting process performance in a thermal energy storage,” *Therm. Sci. Eng. Prog*., vol. 37, no. 2022, p. 101547, 2023, doi: 10.1016/j.tsep.2022.101547.

[19] S. Yaseen, Z. Radhi, R. Natoosh, R. Al-Sabur, R. Homod, and H. Mohammed, “A computational search for the optimal microelectronic heat sink using ANSYS Icepak’’, *International Journal of Thermofluids*, vol. 23, 2024, 100759, https://doi.org/10.1016/j.ijft.2024.100759.

[20] R. Rosli, K. Mohd Annuar, and F. Ismail, “Optimal Pin Fin Heat Sink Arrangement for Solving Thermal Distribution Problem*,” Journal of Advanced Research in Fluid Mechanics and Thermal Sciences*, vol. 11, no. 1, 2015.